이학석사 학위논문

Computational Study on Oxidation of Graphene by Water

물에 의한 그래핀 산화 반응 계산 연구

2021년 8월

서울대학교 대학원
화학부 물리화학전공
손 문 기

Computational Study on Oxidation of Graphene by Water

물에 의한 그래핀 산화 반응 계산 연구

지도교수 손 문 기

이 논문을 이학석사 학위논문으로 제출함

2021년 6월

서울대학교 대학원

화학부 물리화학 전공

손 문 기

손문기의 석사 학위논문을 인준함

2021년 6월

위 원 장 _____ 정 연 준

부위원장 _____ 신 석 민

위 원 _____ 석 차 옥

Abstract

Computational Study on Oxidation of Graphene by Water

Moongi Son
Department of Chemistry
Physical Chemistry
Seoul National University

We performed computational studies on possible oxidation of graphene surface by water molecules. Using density functional theory (DFT) calculations, we investigated the reaction mechanisms for the oxidation of model graphene surfaces, representing pristine graphene and graphene oxide, by water molecules. We also examined the effects of extra charges on the surface and an external electric field on such processes. The results on activation energies showed that the oxidation of pristine graphene with water molecules would not occur easily irrespective of the charged states. It was found that C-O bond formation can be considered to be a major reaction coordinate in reaction of pristine graphene with water. Calculations showed much lower activation energy barrier for the reaction of water molecule with the epoxide group, suggesting that the oxidation reactions by water molecules are much more probable for the graphene oxide than the pristine graphene. It was found the presence of extra charges on the graphene surface may provide alternative reaction paths with an intermediate state by opening the epoxide ring. It can be argued that

the interaction of graphene surfaces with other surfaces or external electric field may influence reactions of water molecules with graphene or graphene oxide by introducing extra charges. It is expected that the results of the present study could provide useful insights and encourage further investigations in order to elucidate the mechanisms of various reactions on graphene.

Keywords: Graphene oxidation, Mechanistic study, Density-functional theory(DFT), Graphene flake
Student Number: 2013-20268

Table of Contents

1 Introduction

Graphene is one of the most popular 2D material in recent decades. For its unique electronic and chemical properties, graphene has attracted fairly high interests in variety of fields[1-5]. It is well known that the pristine graphene itself has a zero band gap by conjugation of unhybridized p_z orbitals of the carbon atoms, which indicates metals-like electronic properties. After the reaction occurs on the basal plane of a graphene, as a result of bond formation, unhybridized p_z orbital turns into sp^3 orbital and no longer contributes to orbital conjugation, which consequently opens the band gap. As controlling of the band gap is important in variety of the fields, several approaches have been applied to tune the electronic and chemical properties of graphene.

Graphene oxide (GO) is one of the most abundant example of functionalized graphene material with open band gap. In addition, graphene oxide is soluble in water, which makes it amenable to bulk production[6,7]. To control the levels of oxidation, GO should be prepared deliberately with various functional groups. The kinds and densities of various functional groups determine the properties of GO. After restoring the sp^2 hybridized orbitals by post processing, the electrical conductivity of reduced graphene oxide (rGO) increases by factor of up to 1000[8-11]. There are however limits with controlled reduction of graphene oxide dispersions with strong acid[12,13]. Though the electrical conductivity increases, it is difficult yet to reduce all of the functional groups and to convert them homogeneously, completely restoring the honeycomb lattice and the sp^2 hybridization. There are many sites with the oxygen functional groups, which are hindered to control the functional groups, because their reaction paths are relying on the location, the type of a bond, and the interaction with solvent molecules[14,15]. They are mainly formed during the oxidation of graphene in various levels[16].

The effective preparation of graphene material would be possible when the detailed mechanisms of oxidation and reduction are well understood. Some experimental results suggested that charge transfer between graphene and substrate or between adsorbate and graphene may be responsible for affecting the chemical response[17-19]. As electrons are injected into or withdrawn from graphene, the Fermi level of graphene can experience changes around the sites. There have been several investigations on the mechanism of oxidation and reduction reaction in graphene[20]. Recently, it was suggested that a pristine graphene is oxidized by triggering of light in the presence of water[21,22]. Graphene is transparent because the electrons in graphene are not excited by the light. As it has been known that photoexcitation leads to a local increase of p-doping for a graphene sheet on a substrate[23,24], it is interesting to understand the underlying processes governing the redox process in order to clarify whether the oxidation of graphene can be influenced by locally constrained charged states,.

In this paper, model reaction between graphene flake and H_2O molecules was studied by performing density functional theory (DFT) calculations on differently charged systems. Moreover, influence of external electric field on a system was also considered to make a comparison with a constrained charge effect on the reaction. Investigation of this reaction would be related with the mechanism of evolution of H_2 by splitting of an H_2O molecule, on graphene or GO being used as catalysts[24].

2 Computational Details

All calculations were performed with GAMESS package[25]. The geometries and energies of the structures are calculated by density functional theory approach, UB3LYP-D3, with an extension of Grimme's dispersion correction[26]. For the basis set, 6-31G(d,p) level was chosen for pristine graphene, while 3-21G(d,p) level was used for graphene with epoxide. Level shift at Fock matrix were considered for Self-Consistent Field stage for the computational convenience. Quadratic approximation were chosen as optimization algorithm, while force matrix were update by Powell's method[27]. Charge density of each atom were obtained by using the classical Mulliken population analysis. Confirmation of transition state between reactant state and product state was obtained by intrinsic reaction coordinate (IRC) algorithm.

3 Results and Discussions

3.1 Oxidation reaction by water molecule on pristine graphene

3.1.1. Reaction of pristine graphene with single water molecule

It is well known that the pristine graphene rarely reacts with water without some other stimulants. However, model study of water molecule reacting with graphene might provide some useful information about various factors involved in such reaction. Small

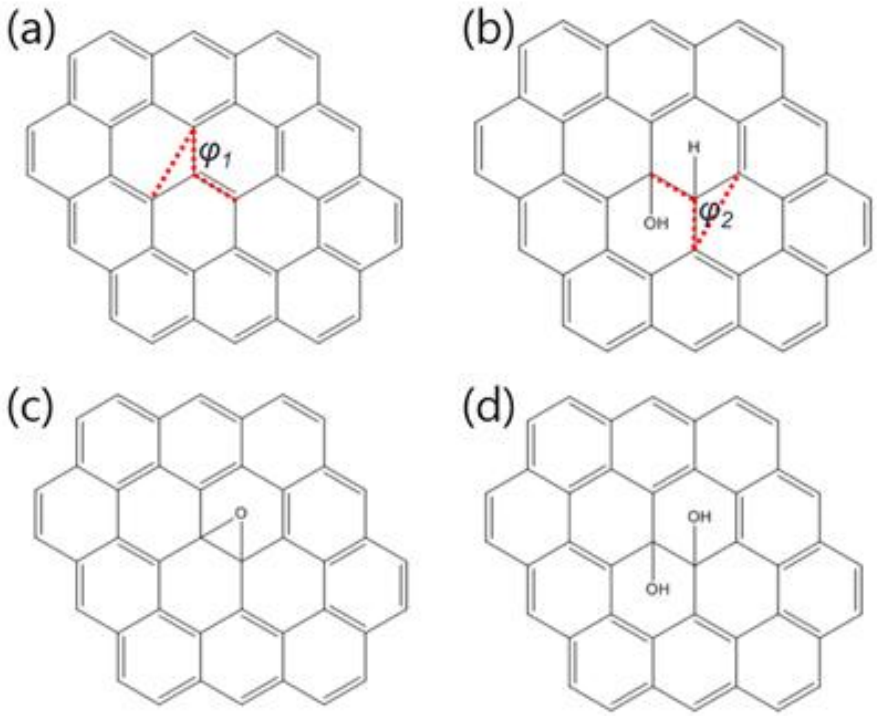

Fig 2. Structure of model graphene used in reaction. (a) Pristine graphene model (b) graphene with one hydroxyl group (c) graphene with an epoxy group at the center bond (d) graphene with two hydroxyl groups at the center bond. φ_1 and φ_2 are improper torsion angles (see Table 1.)

polyaromatic hydrocarbon systems ($C_{42}H_{16}$, see Fig 1) are used as a model graphene. We investigated theoretically the direct reaction between single water molecule and graphene. The optimized

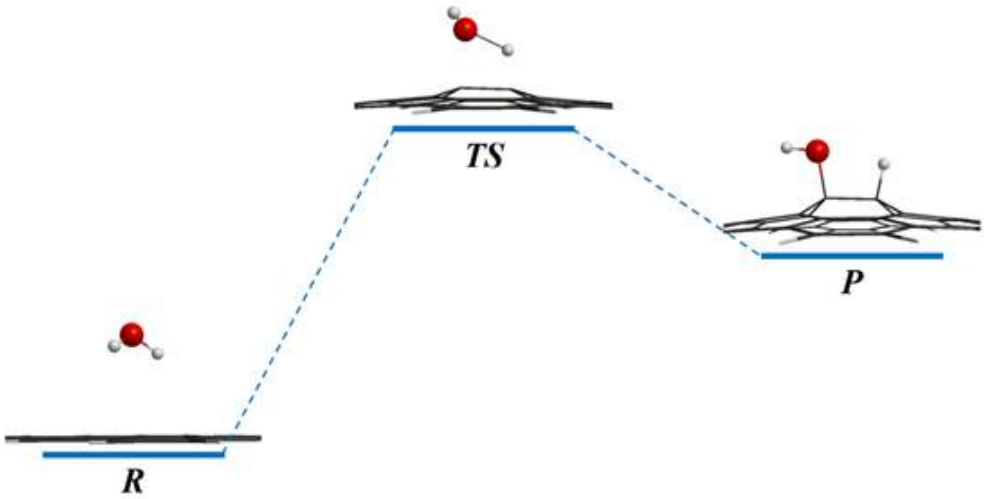

Fig 3. Optimized geometries of graphene and single water molecule involved in reaction in neutral charge. Only H_2O illustrated in ball-stick model, while graphene illustrated in wire frame model.

structures involved in reactions of neutral H_2O with model pristine graphene are shown in Fig 2.

Geometries of initial configuration (R), transition state (TS), and final products (P) of water-graphene reaction were listed in Table 1. From initial to final configurations, both C-O and C-H distances decrease, while O-H distance increases. Changes in initial state geometries showed that charge injection at the graphene may affect the structure of graphene and the physical adsorption behavior of H_2O. The length of C-C bond increased from 1.413 to 1.426(negative) or 1.422(positive), which could suggest weaker bond of graphene with extra charge. H_2O is found to be adsorbed with O atom facing down toward positively charged graphene surface, while H atoms facing down toward surface for neutral or negatively charged graphene. For transition state geometries, bond distances of C-O and C-H showed opposite behavior with extra charge. C-O bond distance is the shortest for positively charged graphene, while C-H bond distance is the shortest for negatively charged graphene. In other words, C-O bond formation may be facilitated with positive

	C-O			C-C			C-H		
	R	TS	P	R	TS	P	R	TS	P
(-)	3.452	2.236	1.481	1.426	1.518	1.556	2.702	1.114	1.104
0	3.184	1.846	1.467	1.413	1.496	1.554	2.706	1.262	1.103
(+)	3.157	1.659	1.46	1.422	1.517	1.555	3.629	1.304	1.108
	O-H			φ_1			φ_2		
	R	TS	P	R	TS	P	R	TS	P
(-)	0.966	2.055	2.079	0.28	11.8	46.03	0	45.27	38.39
0	0.966	1.431	2.076	1.04	27.99	46.08	0.1	23.32	38.72
(+)	0.965	1.38	2.048	0.1	36.29	46.71	0.2	16.67	36.08

Table 1. Geometries (distances in Å, angles in degree) of reactant (R), transition (TS), product state (P) of reaction between graphene and single water molecule at the each charged state. '(-)' stands for negative charge, '0' stands for neutral charge, '(+)' stands for positive charge. φ_1 and φ_2 are improper torsion angles shown in Fig. 1.

charge while negative charged graphene is favorable for C-H bond formation. This conclusion is also supported by dihedral angles, involved with bond forming carbons, as a measure of distortion (see Fig 1). Larger values of ϕ2 for negatively charged state would suggest more distorted C-H bond out of the graphene plane, while larger values of ϕ1 for positively charged state represents similar distortion for C-O bond instead. These results also suggest stronger C-O bond formation in the transition state for positively charged graphene, while stronger C-H bond is formed for positively charged case.

The results on activation energies, as listed in Table 2, suggested that the oxidation of pristine graphene with water molecules would not occur easily irrespective of the charged states. Although the differences are very small, positively or negatively

	R	TS	P
negative	0	71.159	64.068
neutral	0	73.920	54.844
positive	0	67.394	61.500

Table 2. Relative energies compared with each reactant state (R) of transition state (TS), product states (P) in each charged state (Kcal/mol) involved with graphene react with single water molecule.

charged graphene showed lower activation barrier than the neutral graphene. Lower activation energies for the reaction of water molecule with the charged graphene seem to be related with the instability of the reactant configuration as manifested by the increases of C-C bond lengths. Very large reaction energies between the reactant and the product configurations also indicate lower plausibility of the reaction. The distributions of charge densities are compared for the reactant and the transition states of the neutral and the charged graphenes (see Fig. S1). Charge density distributions of the reactant states are similar, as excessive charges can be distributed through delocalized p_z orbitals. The main differences in charge density distributions of transition states are for the carbon (C5) forming a bond with water oxygen. The charge of C5 at the transition state becomes highly negative because charge density moves from water to graphene during the reaction (see Fig. S2).

3.1.2. Reaction of pristine graphene with two water molecules

For a reaction of graphene with single water molecule, water molecule needs to be broken into hydrogen and hydroxide in order to form a bond with graphene. However, such hydrogen and hydroxide

species need not to come from the same water molecule. We investigated the possibility of mechanism for the reaction of graphene with two water molecules. The optimized structures involved in reactions of two H_2O with model pristine graphene are shown in Fig 3.

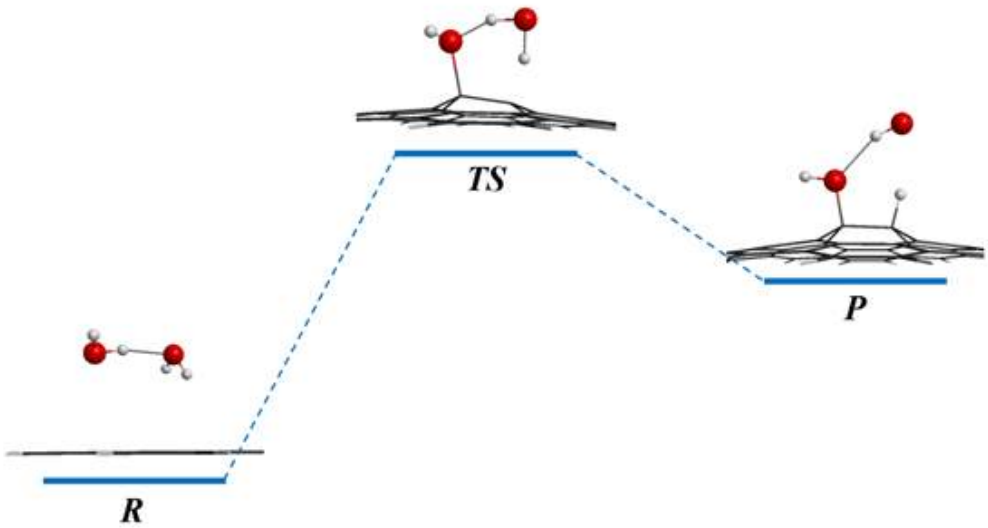

Fig 4. Optimized geometries of graphene and two water involved with reaction in neutral charge. Only H_2O illustrated in ball-stick model, while graphene illustrated in wire frame model.

Geometries of initial configuration (R), transition state (TS), and final products (P) for the reaction of graphene with two water molecules were listed in Table 3. Compared with the geometries of reactions with single water molecule (Table 1), we observed similar trends such that C-O bond distance is the shortest for positively charged graphene, while C-H bond distance is the shortest for negatively charged graphene. However, the differences in bond lengths for differently charged graphene are relatively smaller for the present case with two water molecules. The results on activation energies, as listed in Table 4, showed subtle differences as compared with the reaction involving single water molecule. For the reaction of graphene with two water molecules, the highest barrier is shown for negatively charged graphene while neutral state has the largest

	C-O1			C-H			O1-H		
	R	TS	P	R	TS	P	R	TS	P
(-)	3.456	1.752	1.501	2.775	1.318	1.104	0.974	1.355	1.892
0	3.483	1.636	1.48	2.751	1.38	1.106	0.975	1.43	1.936
(+)	2.94	1.52	1.476	2.967	1.373	1.117	0.975	1.666	1.972

Table 3. Geometries (distances in Å) of transition (TS), final state of reaction between graphene and two water molecule at the each charged state. '(-)' stands for negative charge, '0' stands for neutral charge, '(+)' stands for positive charge.

activation energy for the reaction with single water molecule. It is noted that the activation energies are still very large with the two water molecules involved in the reaction. As C-O bond length shows the largest difference between the reactant and the transition state, C-O bond formation might be suggested as a major reaction coordinate for graphene water reaction. In addition, differently charged graphene exhibited the largest differences in C-O bond lengths for the transition states.

We have investigated the influence of applied electric field on the reaction graphene with two water molecules. The direction of the electric field applied perpendicular to the graphene surface is

	R	TS	P
negative	0.000	82.705	64.068
neutral	0.000	73.920	54.844
positive	0.000	67.394	61.495

Table 4 Relative energies compared with each reactant state (R), transition state(TS), product state (P) in each charged state (Kcal/mol) involved with graphene react with two water molecule.

illustrated in Fig. S3. Positive (+) direction of the electric filed can be considered to be pulling electron density out of the graphene surface, while extra electron density may be added to the surface due to the electric filed in the negative (-) direction. The results on activation energies, as listed in Table 5, showed that the electric filed in the positive direction leads to smaller activation barrier, while larger activation energy is obtained with the electric field in the opposite direction. This result is consistent with the effects of extra charges on the activation energy barriers discussed in the above. It can be concluded that excessive electron density shows higher activation energy barrier while reduced electron density shows lower activation energy barrier for the reaction of pristine graphene with two water molecules.

Field	R	TS	P
-1	0.000	77.622	52.396
0	0.000	73.919	54.843
1	0.000	68.523	56.099

Table 5. Relative energies compared with each reactant state (R) of transition (TS), product state (P) in each charged state (Kcal/mol) involved with graphene react with two water molecules under applied electric field. Unit is in 1 a.u. = 5.142 E+11 V/m.

3.2 Oxidation reaction by water molecule on epoxy group of graphene

We used polyaromatic hydrocarbon systems with epoxide group on its center ($C_{42}H_{16}O$, see Fig. 1) as a model graphene oxide. We performed calculations for the direct reaction between single water molecule and the epoxide group on the graphene. The optimized structures involved in reactions of neutral H_2O with model graphene

oxide are shown in Fig 4.

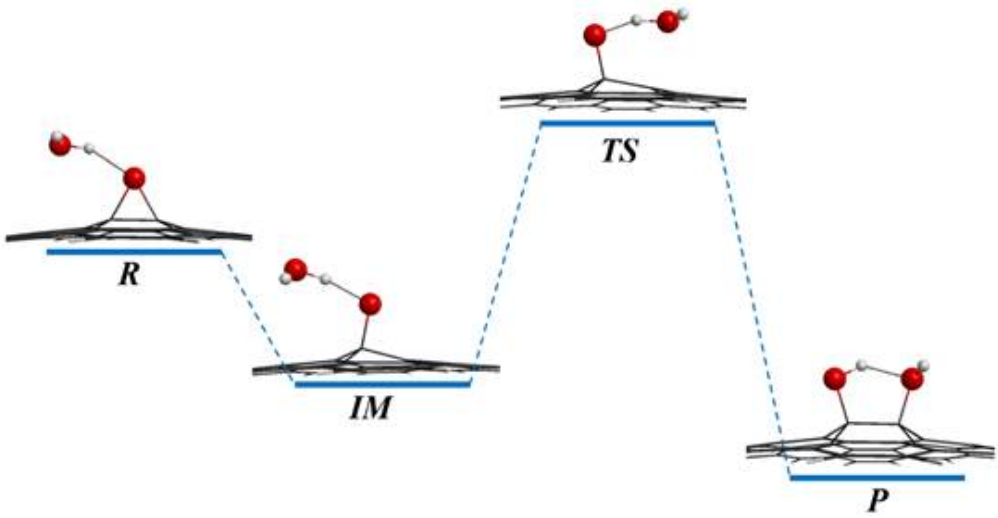

Fig 5. Optimized geometries of graphene with epoxide and water involved in reaction. Most structures achieved from neutral, while intermediate (IM) structure achieved from positive, as IM structure does not exist in neutral. Only H_2O illustrated in ball-stick model, while graphene illustrated in wire frame model.

Relative energies of initial configuration (R), open-ring intermediate state (IM), transition state (TS), and final products (P) for reaction of water molecule with epoxide on graphene were listed in Table 6. It was found that intermediate state with opening of the epoxide ring may exist between the initial state with the closed epoxide and the transition state (Fig 4). Interestingly, such intermediate state with open epoxide ring exist in positively or negatively charged graphene oxide while neutral system does not support the intermediate configuration. The formation of the intermediate state was found to be exothermic process. It can be argued that the initial reaction of water molecule with the epoxide group on the graphene surface may produce easily an intermediate state by opening the epoxide ring for charged graphene oxides. Activation energy barrier for the reaction of water molecule with the neutral graphene oxide, without the intermediate state, was found to

be around 10 kcal/mol. This result suggests that the oxidation reactions by water molecules are much more probable for the graphene oxide with epoxide groups than the pristine graphene. The presence of extra charges on the graphene surface may provide alternative reaction paths involving the intermediate state with open epoxide group, whose activation energies are still lower in the range of 7.3 kcal/mol. It is also noted that the overall reaction of water molecule with the epoxide group on the graphene oxide is exothermic.

	R	IM	TS	P	Ea
negative	0.000	-7.111	0.250	-7.208	7.361
neutral	0.000	-	11.086	-23.616	11.086
positive	0.000	-1.913	5.435	-14.589	7.349

Table 6. Relative energies compared with each reactant state (R), open-ring intermediate state (IM), transition state (TS), product state (P) in each charged state (Kcal/mol) involved with graphene with epoxide react with single water molecule. Activation Energy (Ea) shows the higher energy difference (Kcal/mol) between R to TS and IM to TS

4 Conclusion

We performed DFT calculations to investigate the reaction mechanism for possible oxidation of graphene surface by water molecules. We also examined the effects of extra charges on the surface and an external electric field on such processes. Small polyaromatic hydrocarbon systems ($C_{42}H_{16}$ and $C_{42}H_{16}O$) are used as a model for pristine graphene and graphene oxide. For pristine graphene surface, we investigated the possibility of reaction mechanism with one or two water molecules. The results on activation energies showed that the oxidation of pristine graphene with water molecules would not occur easily irrespective of the charged states. Although the differences are small, positively or negatively charged graphene showed subtle changes in activation barriers compared with the neutral graphene. For the reaction of graphene with two water molecules, the highest barrier is shown for negatively charged graphene while neutral state has the largest activation energy for the reaction with single water molecule. Similar results for the effects of external electric field suggested that activation energy barrier between pristine graphene and water would be affected by the electron density of graphene surface. It is also found that C-O bond formation can be considered to be a major reaction coordinate in reaction of pristine graphene with water.

Activation energy barrier for the reaction of water molecule with the epoxide group was found to be around 10 kcal/mol, suggesting that the oxidation reactions by water molecules are much more probable for the graphene oxide than the pristine graphene. It was also found that the initial reaction of water molecule with the epoxide group on the graphene surface may produce easily an intermediate state by opening the epoxide ring for charged graphene oxides. It can be argued the presence of extra charges on the graphene surface may provide alternative reaction paths with lower

activation energies.

Understanding the detailed mechanism of functionalization of graphene surfaces is a challenging problem. In particular, oxidation of graphene by water molecules may provide an intriguing possibility. Our calculations showed that pristine graphene cannot be easily oxidized by water molecules, confirming general assertions concerning such processes. However, it was demonstrated that presence of epoxide groups, as in graphene oxide surfaces, may provide environments favorable for water oxidation. The present study also illustrates that reactions of water molecules with graphene or graphene oxide can be influenced by the effects of extra charges which may be introduced by the interaction of graphene surfaces with other surfaces or external electric field. We expect that our results could provide useful insights and encourage further investigations in order to elucidate the mechanisms of various reactions on graphene.

Supplementary Figures

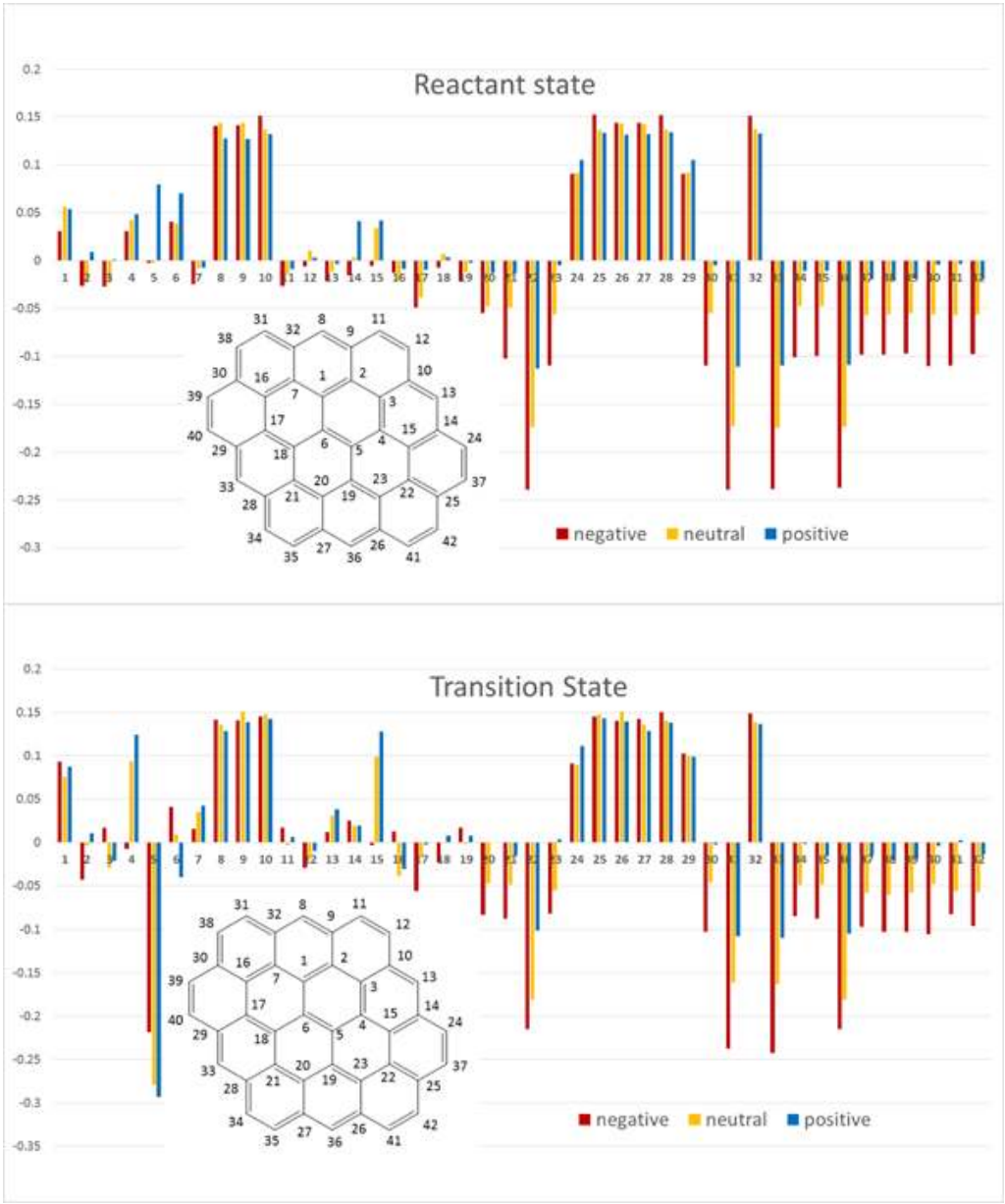

Fig. S1. Charge distribution of graphene is illustrated in (a), (b). Negative (red), neutral (yellow), positive (blue) charged states are illustrated, while (a) illustrates reactant state and (b) illustrates transition state.

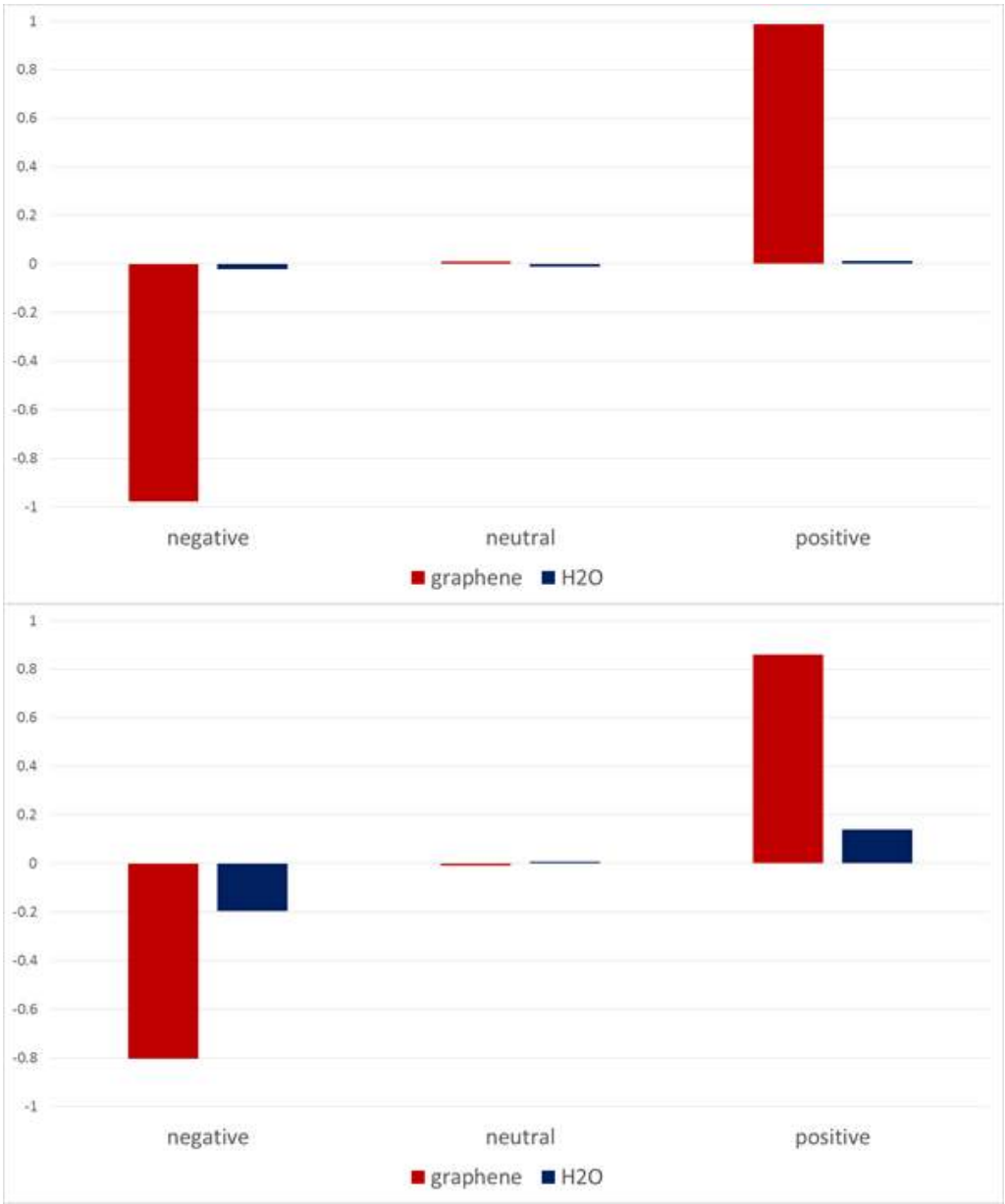

Fig. S2 Charge density of graphene and water is on (c) and (d). Summed charge of graphene (red), H_2O(deep blue) are illustrated in both chart, while © illustrates reactant state and (d) illustrates product state.

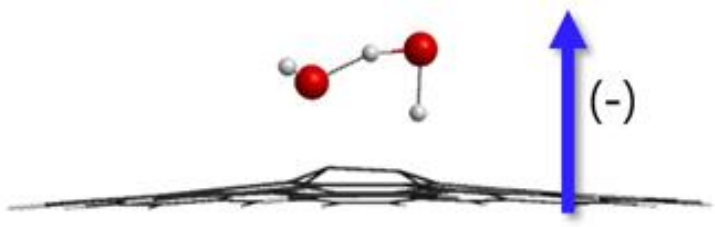

Fig. S3 Transition state of reaction between graphene and two water molecules in neutral charged state with applied field. (-) sign near the blue arrow designates the field direction from graphene plane to water molecules.

References

1. Novoselov KS, Geim AK, Morozov SV, Jiang D, Zhang Y, Dubonos SV, Grigorieva IV, Firsov AA (2004) Electric field effect in atomically thin carbon films. Science 306 (5696):666-669
2. Hamada N, Sawada S, Oshiyama A (1992) New One-Dimensional Conductors - Graphitic Microtubules. Phys Rev Lett 68 (10):1579-1581
3. Novoselov KS, Geim AK, Morozov SV, Jiang D, Katsnelson MI, Grigorieva IV, Dubonos SV, Firsov AA (2005) Two-dimensional gas of massless Dirac fermions in graphene. Nature 438 (7065):197-200
4. Yazyev OV, Helm L (2007) Defect-induced magnetism in graphene. Phys Rev B 75 (12):125408
5. Zheng YS, Ando T (2002) Hall conductivity of a two-dimensional graphite system. Phys Rev B 65 (24):245420
6. Barone V, Hod O, Scuseria GE (2006) Electronic structure and stability of semiconducting graphene nanoribbons. Nano Lett 6 (12):2748-2754
7. Sols F, Guinea F, Castro Neto AH (2007) Coulomb blockade in graphene nanoribbons. Phys Rev Lett 99 (16):166810
8. Jung I, Dikin DA, Piner RD, Ruoff RS (2008) Tunable Electrical Conductivity of Individual Graphene Oxide Sheets Reduced at "Low" Temperatures. Nano Lett 8 (12):4283-4287
9. Gilje S, Han S, Wang M, Wang KL, Kaner RB (2007) A chemical route to graphene for device applications. Nano Lett 7 (11):3394-3398
10. Gomez-Navarro C, Weitz RT, Bittner AM, Scolari M,

Mews A, Burghard M, Kern K (2007) Electronic transport properties of individual chemically reduced graphene oxide sheets. Nano Lett 7 (11):3499-3503

11. Zhou M, Wang YL, Zhai YM, Zhai JF, Ren W, Wang FA, Dong SJ (2009) Controlled Synthesis of Large-Area and Patterned Electrochemically Reduced Graphene Oxide Films. Chem-Eur J 15 (25):6116-6120
12. Tung VC, Allen MJ, Yang Y, Kaner RB (2009) High-throughput solution processing of large-scale graphene. Nat Nanotechnol 4 (1):25-29
13. Ren PG, Yan DX, Ji X, Chen T, Li ZM (2011) Temperature dependence of graphene oxide reduced by hydrazine hydrate. Nanotechnology 22 (5):055705
14. Liu H, Lee JY (2013) Electric field assisted oxygen removal from the basal plane of the graphitic material. J Comput Chem 34 (4):305-310
15. Park H, Lee JY, Shin S (2014) Computational Study on Removal of Epoxide from Narrow Zigzag Graphene Nanoribbons. J Phys Chem C 118 (46):27123-27130
16. Solis-Fernandez P, Paredes JI, Villar-Rodil S, Guardia L, Fernandez-Merino MJ, Dobrik G, Biro LP, Martinez-Alonso A, Tascon JMD (2011) Global and Local Oxidation Behavior of Reduced Graphene Oxide. J Phys Chem C 115 (16):7956-7966
17. Leenaerts O, Partoens B, Peeters FM (2008) Adsorption of H(2)O, NH(3), CO, NO(2), and NO on graphene: A first-principles study. Phys Rev B 77 (12):125416
18. Yavari F, Kritzinger C, Gaire C, Song L, Gullapalli H, Borca-Tasciuc T, Ajayan PM, Koratkar N (2010) Tunable Bandgap in Graphene by the Controlled Adsorption of Water Molecules. Small 6 (22):2535-2538
19. Schedin F, Geim AK, Morozov SV, Hill EW, Blake P,

Katsnelson MI, Novoselov KS (2007) Detection of individual gas molecules adsorbed on graphene. Nat Mater 6 (9):652-655

20. Dimiev AM, Alemany LB, Tour JM (2013) Graphene Oxide. Origin of Acidity, Its Instability in Water, and a New Dynamic Structural Model. Acs Nano 7 (1):576-588

21. Zhang LM, Diao SO, Nie YF, Yan K, Liu N, Dai BY, Xie Q, Reina A, Kong J, Liu ZF (2011) Photocatalytic Patterning and Modification of Graphene. J Am Chem Soc 133 (8):2706-2713

22. Wang XJ, Zou LP, Li D, Zhang QC, Wang FL, Zhang ZX (2015) Photo-Induced Doping in Graphene/Silicon Heterostructures. J Phys Chem C 119 (2):1061-1066

23. Alexeev E, Moger J, Hendry E (2013) Photo-induced doping and strain in exfoliated graphene. Appl Phys Lett 103 (15):151907

24. Singh GP, Shrestha KM, Nepal A, Klabunde KJ, Sorensen CM (2014) Graphene supported plasmonic photocatalyst for hydrogen evolution in photocatalytic water splitting. Nanotechnology 25 (26):265701

25. Schmidt MW, Baldridge KK, Boatz JA, Elbert ST, Gordon MS, Jensen JH, Koseki S, Matsunaga N, Nguyen KA, Su SJ, Windus TL, Dupuis M, Montgomery JA (1993) General Atomic and Molecular Electronic-Structure System. J Comput Chem 14 (11):1347-1363

26. Grimme S, Antony J, Ehrlich S, Krieg H (2010) A consistent and accurate ab initio parametrization of density functional dispersion correction (DFT-D) for the 94 elements H-Pu. J Chem Phys 132 (15)

27. Powell MJD (1964) An efficient method for finding the minimum of a function of several variables without calculating derivatives. The Computer Journal 7

(2):155-162

국문초록

이 논문에서는 그래핀 표면에서 물에 의한 산화 반응에 대하여 계산화학적으로 접근하였다. 밀도범함수이론(DFT) 계산을 이용하여 그래핀과 산화그래핀(Graphene oxide)의 모델로 잡은 그래핀 조각(Graphene flake)이 물에 의해 산화되는 반응 메커니즘에 대하여 계산하였다. 특히, 이 산화과정에 대하여 그래핀에 분포하는 추가전하나 외부 전기장에 따라 어떠한 영향이 있는지에 대하여 연구하였다. 순수한 그래핀을 모델링한 그래핀 조각의 경우 그래핀에 분포한 전화와 상관없이 물에 의한 산화가 거의 일어나지 않을 것으로 나타났지만 산화그래핀을 모델링한 에폭시 그룹이 있는 그래핀 조각의 경우 반응 메커니즘에서의 활성화 에너지가 비약적으로 낮아질 뿐 아니라 전하 분포에 따라 훨씬 낮은 활성화 에너지를 갖을 것으로 예측하였다. 순수한 그래핀을 모델링한 그래핀 조각의 경우 C-O 결합이 생성되는 과정이 주요 반응 좌표(Reaction coordinate)로 제시되었지만, 산화그래핀을 모델링한 에폭시 그룹이 있는 조건에서는 전하 분포에 따라 에폭시 고리가 열린 형태의 중간체를 갖는 다른 반응 좌표를 따라가며 낮은 활성화 에너지를 갖는다. 이것으로 그래핀이 다른 물질의 표면에 붙어있을 때 외부 전기장으로 인하여 산화에 영향을 받는 이유를 그래핀 표면에 추가 전하가 분포하기 때문인 것으로 설명할 수 있다. 이 연구로 인하여 향후 그래핀의 산화와 관련된 반응 메커니즘을 밝히는 연구에 도움이 되길 기대한다.

주요어: 그래핀 산화, 반응 메커니즘 연구, 밀도범함수이론(DFT), 그래핀 조각

학번 : 2013-20268

Appendix

Automated reaction network construction for NHC catalyzed benzoin condensation reaction

1 Introduction

It is often useful to construct a comprehensive chemical kinetic model, especially for complex systems involving combustion, catalytic reaction, or environmental process. However, most of these model only depend on well-known reaction paths [1], while it is more likely that system with complex reaction chemistry would have alternative reaction path which is unknown. It is suggested that even a single new reaction added on these kinetic model could significantly increases their reliability [2]. If we want to construct reliable chemical kinetic model, systematic search of all the possible reactions of the system is essential.

Breslow intermediate derived from N-heterogenous carbenes (NHC) is one of the hot topics in the mechanistic study [1]. First postulated in 1958 [2], most attempts to detect Breslow intermediates only resulted in finding their derivatives [3-4]. Recently, M. Paul et al. separated and detected Breslow intermediates with NMR [5] under strict conditions. However, a lot of interest still persist on understanding the actual mechanism involved in NHC catalyzed reaction [6,11]. One of the reason would be that it is almost impossible to observe full reaction pathway in real time. Even though Breslow intermediate was succesfully separated in certain conditions, we cannot guarantee actual reaction goes through the detected intermediate in a specific reaction path. The well-organized mechanism of NHC catalyzed benzoin condensation reaction, as proposed computationally by Hsieh et al. [7], illustrated an active interest on this topic.

As mechanistic study involved in the Breslow intermediate is still posing new questions [8], more thorough investigation on the mechanism would provide more insight understanding the involved reactions. Automated reaction path finder is one of the promising approaches [9-11]. Many studies using automated reaction path

finding methods have tried to predict the detailed reaction mechanisms. Recently, many successful results have been obtained from the automated searching approach, not only predicting known pathways but also suggesting unknown but theoretically reasonable pathways.

In the present study, NHC (3-methylthiazole) catalyzed benzoin condensation reaction is investigated with the automated reaction path finder. We analyzed not only the well-accepted mechanism, but also other alternative reaction pathways obtained by the reaction network search.

2 Computational Details

To include reaction paths predicted from previous studies [3-7,12], 3 Benzaldehyde molecules and 2 NHC catalyst molecules are explicitly included in the reaction network searching. Network extraction is done by the ACE-reaction program [11]. For intermediate sampling by the ACE-reaction, active atoms need to be chosen. Starting molecules and their active atoms are illustrated in Fig 1. In the present study, all bond breaking reactions are considered as heterolytic bond breaking, while some of the previous studies considered homolytic bond breaking mechanism [11]. 2nd shortest path is also included as a possible reaction pathway, as the most promising reaction path from human insight is rather detouring route in the concept of chemical distance used in the ACE-reaction

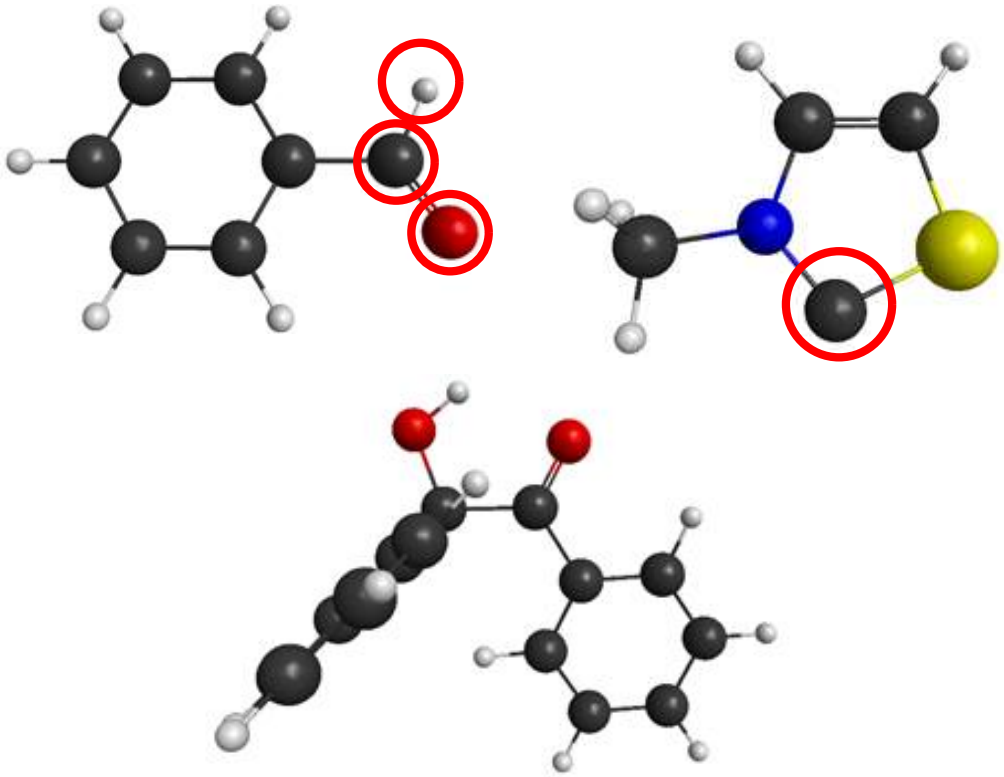

Fig 1. Benzaldehyde (left) and 3-methylthiazole (right) as a NHC catalyst, as well as product molecule of benzoin (below) are illustrated. Active atoms are marked as circles.

program. Digression factor is chosen as 4 for moderate number of intermediates sampling.

To confirm the stability of the intermediates and make use of their state properties, quantum mechanical calculations are performed on all of the related species. Calculations are done with G09 package [13] using M06-2X/6-31+G(d,p) level computation. IEFPCM method is used for implicit solvent as methanol.

3 Result and Discussions

Reaction network extracted from the model system, with 3 benzaldehyde and 2 NHC catalyst molecules, is shown in Fig 2. Several attempts were done for choosing appropriate network size. Each of the vertices represents a possible intermediate or reactant/product, while eachof the edges represents a single reaction step.

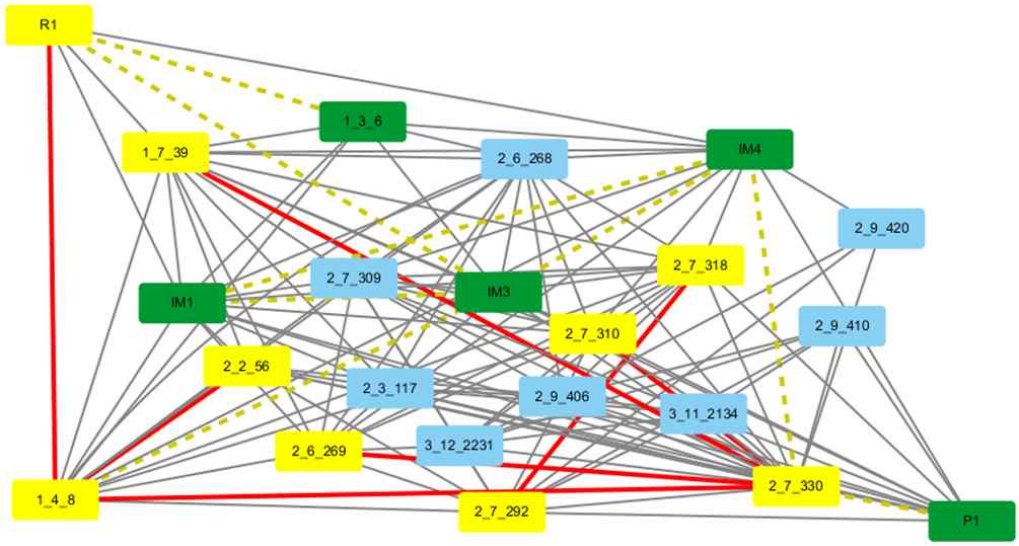

Fig 2. Extracted reaction network by ACE-reaction program. Reaction paths suggested by other mechanisms are illustrated with dashed line.

It is noted that some of the reaction paths suggested by human insights could be excluded only with the network selection process. Gronert, S suggested a reaction pathway involving spiro-epoxide intermediate in 2007[12]. One of the intermediates on the reaction pathway was found to be too unstable to occur (Fig 3.). Alternatively, automated path finder recommended other plausible pathways involving spiro-epoxide intermediates. Within the propsed mechanisms, spiro-epoxide intermediates may provide plausible reaction paths which are linked to the well-known mechanism including observed intermediates.

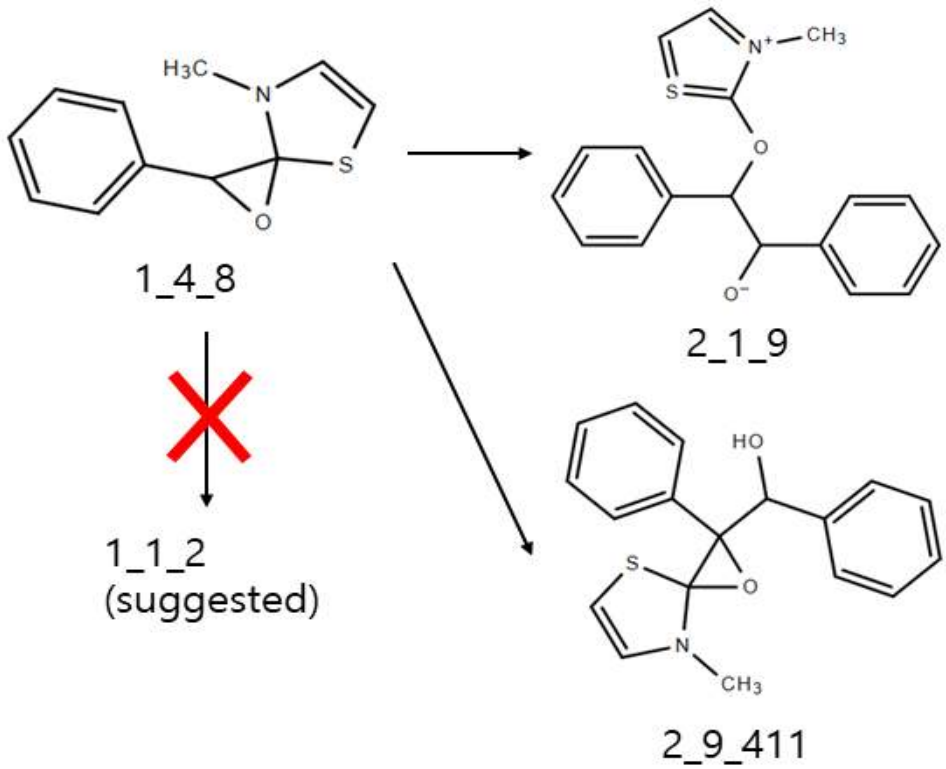

Fig 3. Part of extracted reaction network involving spiro-epoxide species. Originally suggested intermediate is excluded due to low stability, while other plausible intermediates are proposed.

Wanzlick equilibrium or protonated NHC is also included in the reaction network. It is suggested from the previous study that dimerization or protonation of NHC contributes to decrease in catalytic power [1]. In the resulting reaction network, those intermediates not only contribute to alternative paths but may also show high stability, thus hindering further reaction from stable intermediates.

Regarding the well-known breslow mechanism, the resulting reaction network proposed a kind of shortcut, which excludes the breslow intermediate from the reaction mechanism (Fig 4.). As the reaction path finder does not rely on well-known organic chemistry reactions, it prefers a reaction path without redundant formation or breaking of bonds. Since the program takes every bonds equally, hydrogen shift reaction would be highly undesirable, while it

frequently occurs in actual experiments.

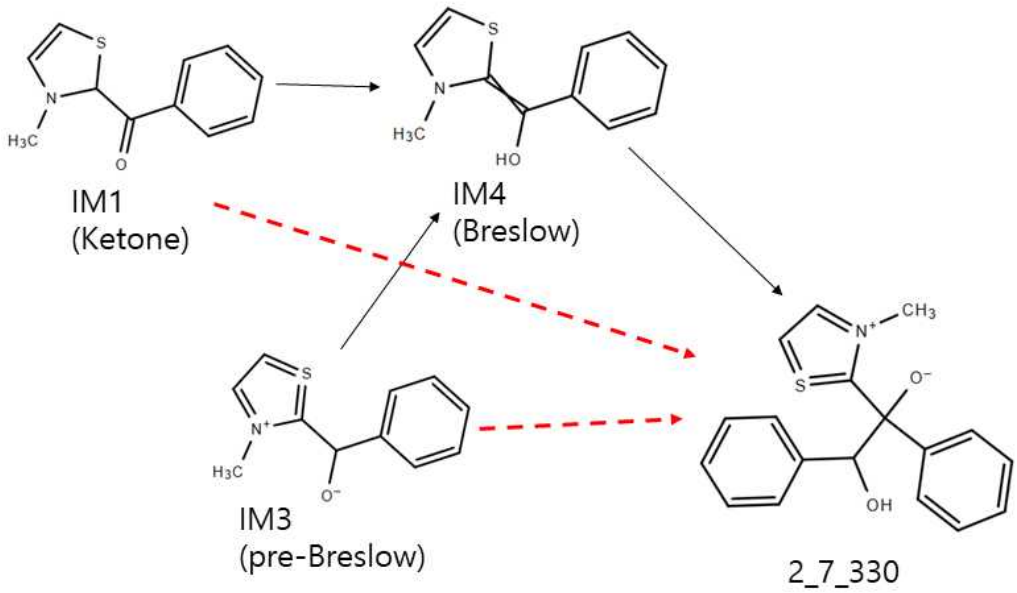

Fig 4. Part of extracted reaction network comparing mechanism suggested in other studies (full arrow) and that proposed in the present study (dashed arrow).

4 Conclusion

The mechanism of benzoin condensation reaction was investigated with the automated reaction path finding tool, ACE-reaction. As most reaction paths from human intuition can be included in automatically searched one, the present study would provide some useful insight on the advatages of using automated reaction path finder. Contrary to the knowledge based methods, the present method could provide diverse possibilities including well-known mechanisms. The program could provide alternative path with stable intermediates while excluding unstable intermediates, or investigate subsequent reactions of well-known stable intermediates. The concept of chemical distance could provide efficient approach for constructing model reaction networks, while it could overestimate hydrogen shift reaction and exclude several plausible reaction paths.

There are several limitations for the current approach. Firstly, reaction path only includes heterolytic bond cleavage, while several evidences suggest involvement of radical species in reaction mechanisms [7]. Although most reactions concern only heterolytic bond cleavage, homolytic bond cleavage should be considered to compare with well-known mechanisms. Additionally, further computations are necessary to confirm actual reaction mechanisms. The reaction network extraction only suggests possible reactions, therefore, confirmation of the real reaction transition states would require much more computations. However, it can be argued that automated reaction path finder could sort out most of the plausible reaction mechanisms without chemical intuition, even in the absence of high demanding transition state computations.

Supplementary Figures

List of plausible intermediates

1_3_6

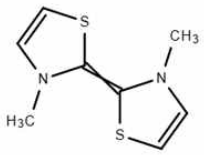

3_11_2134

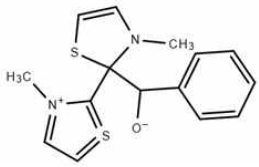

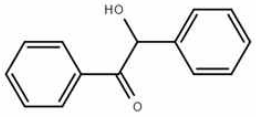

3_11_2159

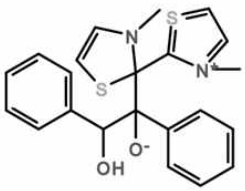

3_2_280

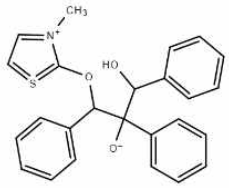

2_6_268

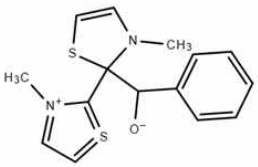

2_3_117

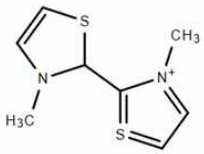

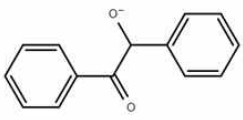

1_7_39

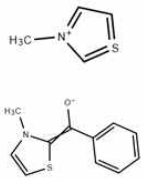

2_9_406

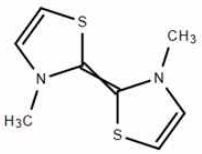

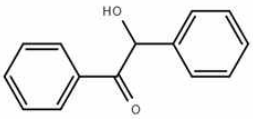

2_1_21

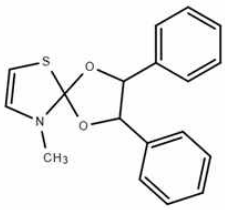

2_2_56

2_1_9

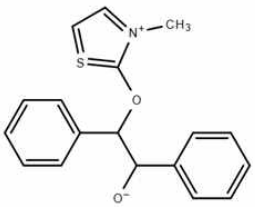

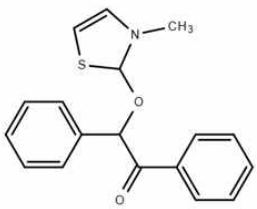

2_7_309

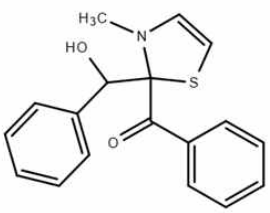

2_7_318

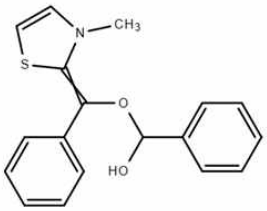

2_7_330

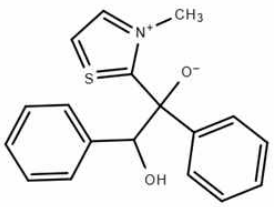

2_9_411

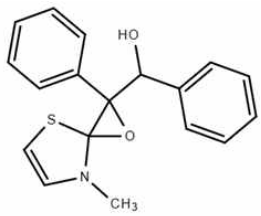

3_12_2231

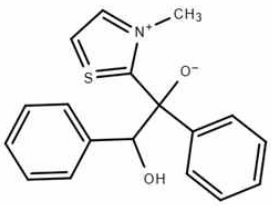

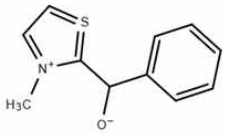

1_11_22

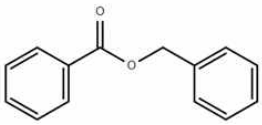

2_6_269

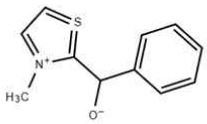

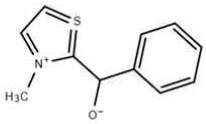

1_4_7

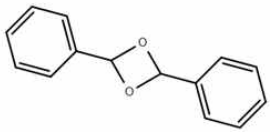

2_3_114

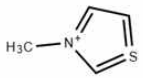

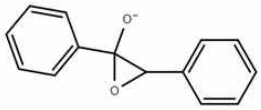

2_9_420

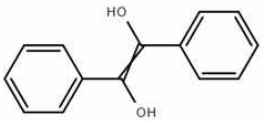

1_1_33

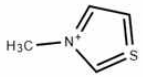

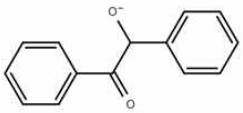

2_10_437

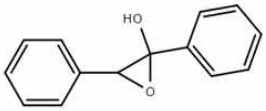

2_7_310

P1

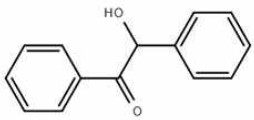

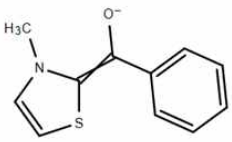

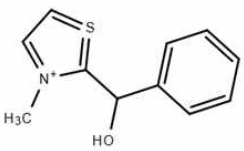

IM1

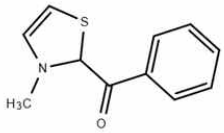

2_7_291

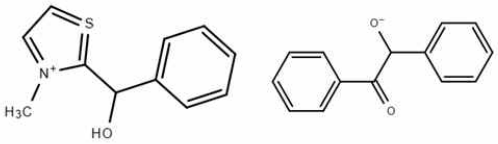

IM3

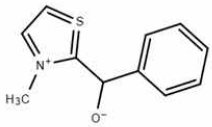

2_7_292

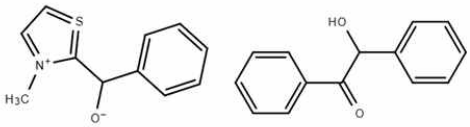

IM4

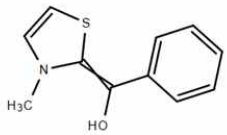

2_9_410

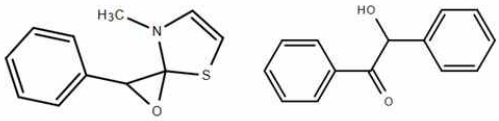

1_4_8

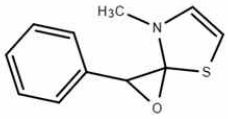

2_3_120

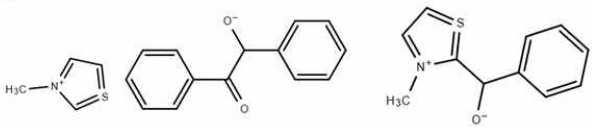

2_8_361

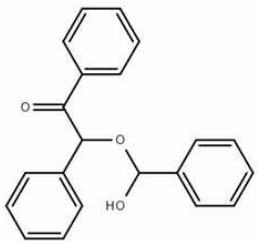

2_9_416

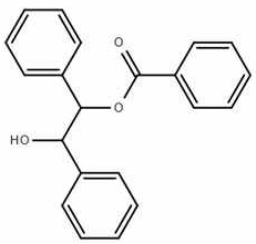

2_9_412

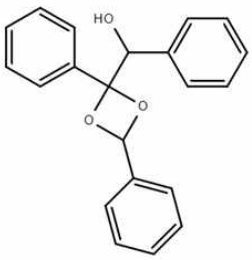

2_3_119

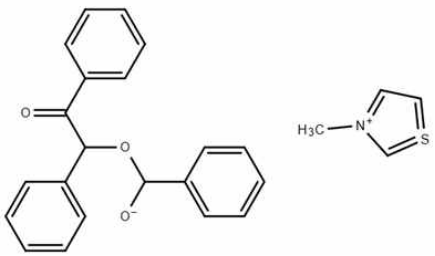

Table of Suggested intermediates

Intermediates (IMs) spanned from reactants and active atoms. Unit of energy (E) is Kcal/mol, compared to reactant state. Several intermediates are too unstable that bonds spontaneously break (marked with -). Most intermediates are too unstable to reaction occurs, while some intermediates are too stable that it would actually disturb reaction occurs as predicted.

IMs	E	IMs	E
1_11_21	33.47703	2_1_9	20.59425
1_11_22	-11.4251	2_2_52	55.86784
1_11_43	50.69967	2_2_53	59.66302
1_12_23	78.74309	2_2_56	-3.12061
1_1_2	40.24724	2_2_60	139.6624
1_1_33	19.41579	2_2_71	133.1187
1_2_34	64.68185	2_2_73	87.97251
1_3_6	-13.3854	2_2_74	90.94691
1_4_7	23.73117	2_2_79	89.1127
1_4_8	6.438253	2_2_84	-
1_7_39	5.433609	2_2_85	110.3144
2_10_437	15.62061	2_2_87	28.94139
2_10_452	65.35768	2_2_88	128.713
2_10_472	114.3806	2_3_110	65.04831
2_16_737	66.01719	2_3_114	17.00176
2_1_21	-9.65361	2_3_117	9.512424
2_1_2	80.49447	2_3_119	18.98908
2_1_41	26.65349	2_3_120	24.18298
2_1_4	39.42143	2_3_126	29.01041
2_1_8	45.01443	2_5_209	218.2166

IMs	E	IMs	E
2_6_268	3.212851	2_9_412	23.12688
2_6_269	9.534387	2_9_416	-10.4788
2_6_287	35.09224	2_9_420	9.696912
2_7_291	21.031	3_1_118	34.56262
2_7_292	4.355547	3_11_2134	2.801205
2_7_309	-3.29882	3_11_2159	15.27861
2_7_310	7.04882	3_12_2231	10.65575
2_7_312	57.1122	3_1_28	69.18172
2_7_313	55.46686	3_1_99	39.00979
2_7_318	1.169679	3_2_204	35.42419
2_7_325	94.43461	3_2_240	46.13579
2_7_328	-	3_2_266	73.21285
2_7_330	5.888554	3_2_280	15.90048
2_8_358	62.26782	3_2_297	30.88855
2_8_359	51.29643	3_4_731	62.75665
2_8_361	8.113077	IM1	-8.5197
2_9_391	263.4827	IM3	4.767193
2_9_406	-13.7971	IM4	-3.48268
2_9_410	6.026606	P1	-0.41165
2_9_411	14.29154	R1	0

References

1. Feroci, M., Chiarotto, I., & Inesi, A. (2016). Advances in the knowledge of N-Heterocyclic carbenes properties. The backing of the electrochemical investigation. Catalysts, 6(11), 178.
2. Breslow, R. (1958). On the mechanism of thiamine action. IV. 1 Evidence from studies on model systems. Journal of the American Chemical Society, 80(14), 3719-3726.
3. Berkessel, A., Elfert, S., Etzenbach Effers, K., & Teles, J. H. (2010). Aldehyde umpolung by N heterocyclic carbenes: NMR characterization of the Breslow intermediate in its keto form, and a spiro dioxolane as the resting state of the catalytic system. Angewandte Chemie International Edition, 49(39), 7120-7124.
4. DiRocco, D. A., & Rovis, T. (2012). Catalytic Asymmetric Cross Aza Benzoin Reactions of Aliphatic Aldehydes with N Boc Protected Imines. Angewandte Chemie, 124(24), 6006-6008.
5. Paul, M., Sudkaow, P., Wessels, A., Schlörer, N. E., Neudörfl, J. M., & Berkessel, A. (2018). Breslow Intermediates from Aromatic N Heterocyclic Carbenes (Benzimidazolin 2 ylidenes, Thiazolin 2 ylidenes). Angewandte Chemie International Edition, 57(27), 8310-8315.
6. (a) Bielecki, M., & Kluger, R. (2017). The Need for an Alternative to Radicals as the Cause of Fragmentation of a Thiamin Derived Breslow Intermediate. Angewandte Chemie, 129(22), 6418-6420. (b) Alwarsh, S., Xu, Y., Qian, S. Y., & McIntosh, M. C. (2016). Radical [1, 3] Rearrangements of Breslow Intermediates. Angewandte Chemie International Edition, 55(1), 355-358.
7. Hsieh, M. H., Huang, G. T., & Yu, J. S. K. (2018). Can the Radical Channel Contribute to the Catalytic Cycle of N-Heterocyclic Carbene in Benzoin Condensation?. The

Journal of organic chemistry, 83(24), 15202-15209.

8. Cao, S., Yuan, H., & Zhang, J. (2019). A mechanistic investigation into N-heterocyclic carbene (NHC) catalyzed umpolung of ketones and benzonitriles: is the cyano group better than the classical carbonyl group for the addition of NHC?. Organic Chemistry Frontiers, 6(4), 523-531.

9. Grambow, C. A., Jamal, A., Li, Y. P., Green, W. H., Zador, J., & Suleimanov, Y. V. (2018). Unimolecular reaction pathways of a γ-ketohydroperoxide from combined application of automated reaction discovery methods. Journal of the American Chemical Society, 140(3), 1035-1048.

10. Dewyer, A. L., Argüelles, A. J., & Zimmerman, P. M. (2018). Methods for exploring reaction space in molecular systems. Wiley Interdisciplinary Reviews: Computational Molecular Science, 8(2), e1354.

11. Kim, J. W., Kim, Y., Baek, K. Y., Lee, K., & Kim, W. Y. (2019). Performance of ACE-reaction on 26 organic reactions for fully automated reaction network construction and microkinetic analysis. The Journal of Physical Chemistry A, 123(22), 4796-4805.

12. Gronert, S. (2007). An epoxide intermediate in nucleophilic acylations by thiazolium precursors. Organic letters, 9(16), 3065-3068.

13. Gaussian 09, Revision D.04, M. J. Frisch, G. W. Trucks, H. B. Schlegel, G. E. Scuseria, M. A. Robb, J. R. Cheeseman, G. Scalmani, V. Barone, G. A. Petersson, H. Nakatsuji, X. Li, M. Caricato, A. Marenich, J. Bloino, B. G. Janesko, R. Gomperts, B. Mennucci, H. P. Hratchian, J. V. Ortiz, A. F. Izmaylov, J. L. Sonnenberg, D. Williams-Young, F. Ding, F. Lipparini, F. Egidi, J. Goings, B. Peng, A. Petrone, T. Henderson, D. Ranasinghe, V. G. Zakrzewski, J. Gao, N. Rega, G. Zheng, W. Liang, M. Hada, M. Ehara, K. Toyota, R. Fukuda, J. Hasegawa, M. Ishida, T. Nakajima, Y. Honda, O. Kitao, H. Nakai, T.

Vreven, K. Throssell, J. A. Montgomery, Jr., J. E. Peralta, F. Ogliaro, M. Bearpark, J. J. Heyd, E. Brothers, K. N. Kudin, V. N. Staroverov, T. Keith, R. Kobayashi, J. Normand, K. Raghavachari, A. Rendell, J. C. Burant, S. S. Iyengar, J. Tomasi, M. Cossi, J. M. Millam, M. Klene, C. Adamo, R. Cammi, J. W. Ochterski, R. L. Martin, K. Morokuma, O. Farkas, J. B. Foresman, and D. J. Fox,